







Estimating the Heat Flow, Geothermal Gradient and Radiogenic Heat within the Young Granites of Jos Plateau North Central Nigeria

Adetona, A. A.¹  | Rafiu, A. A.¹  | Aliyu, B. Sh.¹  | John, M. K.¹  | Kwaghghua, I. F.¹  

1. Department of Geophysics, Faculty of Physical Science, Federal University of Technology Minna, Minna, Nigeria.

Corresponding Author E-mail: fidelisik@gmail.com

(Received: 1 July 2023, Revised: 9 Dec 2023, Accepted: 9 Jan 2024, Published online: 20 Feb 2024)

Abstract

Both aeromagnetic and radiometric data were used to evaluate the Curie point depth and radiogenic heat production (RHP) of the young granitic regions of the Jos Plateau. An area of 55 by 110 square kilometers is bounded by latitude 9°30' to 10°00' N and longitude 8°30' to 9°30' E in central Nigeria. The magnetic data was subjected to spectral analysis to obtain the Curie depth, which was subsequently used to evaluate the geothermal gradient and heat flow for the area. Also, the concentration of radioelements (potassium, thorium and uranium) and the average density of the in-situ rock were used to estimate the radiogenic heat production at each point where the Curie point was evaluated. The heat flow in the study area ranges from 10 to 165.5 mW/m² with an average value of 111.00 mW/m². The regions with anomalous heat flow of 165.5 mW/m² are located around Bowon Dodo, Dan Tsofo, Kadunu, Gimi, Kaura and Zankan in plateau state. The geothermal gradient values range from 5 to 68 °C/Km with an average of 26.16 °C/Km. The radiometric data analysis resulted in radiogenic heat values ranging from 0.4 μW/m³ to 6 μW/m³ with an average radiogenic heat value of 3.36 μW/m³. Both analyses revealed that regions such as Ataka, Gimi, Jimjim and Pari could be investigated for geothermal energy potential. The high concentration of uranium, thorium and potassium associated with the study area is likely due to the weathering of the in-situ granitic basement rocks.

Keywords: Curie point depth, heat flow, geothermal gradient, radiogenic heat production.

1. Introduction

Geothermal energy is a form of natural renewable energy that is generated and stored in the earth. The origin of the Earth's geothermal energy includes the radioactive disintegration of minerals, volcanic activity, and solar energy absorbed at the surface. Among these sources, the radioactive decay of radioelements contributes a major quota to the internal warming of the Earth (Davies, 1980; McCay et al., 2014; Kuforijimi and Aigbogun, 2017; Adagunodo et al., 2019; Adetona et al., 2023).

The Curie-point depth (CPD) is useful for studying the subsurface temperature, geothermal gradients, and heat flow. This is important for understanding the thermal maturation of sediments and past thermal regimes in a basin. CPD has been used by various researchers to estimate the depth to the bottom of magnetic sources where the Curie temperature can be accessed (Okubo et al., 1985; Tanaka et al., 1999; Nuri et al., 2005; Trifonova et al., 2009; Maden, 2010; Adetona et al., 2017; Nwankwo and Sunday,

2017; Nwankwo et al., 2009; Salako et al., 2020; Raj et al., 2020; Adetona et al., 2023).

The depth at which the dominant magnetic mineral in the crust passes from a ferromagnetic state to a paramagnetic state under the effect of increasing temperature is known as the Curie point depth (CPD) (Nagata, 1961). The deeper the Curie point depth, the lower the heat flow in a given region, while the shallower region corresponds to higher heat flow. The Curie temperature ranges from a few hundred to 580 °C for titanomagnetite, which is the magnetic mineral that is very common in igneous rocks. According to Nuri et al. (2005), geothermally active areas are typically associated with shallow Curie point depths. The geothermal gradient refers to the difference in temperature between the planet's core and its surface, which drives a continuous conduction of thermal energy in the form of heat from the core to the surface that is about 1 °C km⁻¹ on average (Lowrie and Fichtner, 2020).

Cite this article: Adetona, A. A., Rafiu, A. A., Aliyu, B. Sh., John, M. K., & Kwaghghua, I. F. (2024). Estimating the Heat Flow, Geothermal Gradient and Radiogenic Heat within the Young Granites of Jos Plateau North Central Nigeria. *Journal of the Earth and Space Physics*, 49(4), 69- 81. DOI: <http://doi.org/10.22059/jesphys.2024.361557.1007538>

E-mail: (1) tonabass@gmail.com | iyiolarafiu@futminna.edu.ng | shakirat@futminna.edu.ng | kanamoses12@gmail.com



The average heat flow is about 60 mWm^{-2} in thermal normal continental regions; Values between $80\text{-}100 \text{ mWm}^{-2}$ are good indicators of viable geothermal sources. However, values greater than 100 mWm^{-2} show anomalous conditions (Cull and Conley, 1983; Jessop et al., 1976). This research aims to analyze aeromagnetic and radiometric data using spectral analysis and examining radiogenic heat production. The result of the heat flow and geothermal gradient from spectral analysis is then correlated with the radiogenic heat production within the study area to investigate the favorability and location for geothermal energy exploration.

2. Location of the Study Area

The Naraguta sheet area comprises the following towns: Jos, Bukuru, Vom, BarkinLadi, Rukuba, Foron, Miango, Kigom, Ganawuri located in Plateau state, North Central Nigeria. It is bounded by longitude $8^{\circ}30'$ to $9^{\circ}00'$ N and latitude $9^{\circ}30'$ to $10^{\circ}00'$ E and covering an area of about 2970 km^2 . The study area has high relief features, with elevations ranging from 1800 m to 5300 m above sea level. Maijuju is located between longitude $9^{\circ} 00' \text{ E}$ to $9^{\circ} 30' \text{ E}$ and latitude $9^{\circ} 30' \text{ N}$ to $10^{\circ} 00' \text{ N}$. The study area covers approximately 2970 km^2 and covers Jarawa, shere, shona, jimjim, Wai, bijim, Gohzi, Lere,

Girim, Langai, Maijuja, Fedaki, Maigemu and Gora. It is accessible by road and several footpaths, and river channels connected to the study area. The mapping of the study area location is shown in Figure 1.

2-1. Geology of the Study Area

The Jos Plateau is dominated by three types of rock: basement Rocks, younger granite rocks and basalts or basaltic rocks. Its forming includes distinctive groups of intrusive and volcanic rocks, bounded by ring dykes or faults (Macleod et al., 1971). Several years ago, volcanic activities created a vast basaltic plateau and volcanoes, resulting in regions of mainly narrow and deep valleys, as well as sediments from the middle of rounded hills with shear facies. Other rocks found in the area include basic rocks (Gabbro and Dolerite) and basement rocks such as migmatite, which are resistant to erosion. Figure 2 shows the geological maps of Naraguta (sheet 168) and Maijuju (sheet 169), respectively. The most common mineral in the area is cassiterite. Other minerals in the area include columbite, wolfram, pyrochlore, fergusonite, thorite, zircon, monazite, xenotime, beryllium minerals, molybdenite, cryolite, and other minor minerals such as topaz, gelana, pyrite, arsenopyrite, bismuthine, and chalcopyrite (Obaje, 2009).

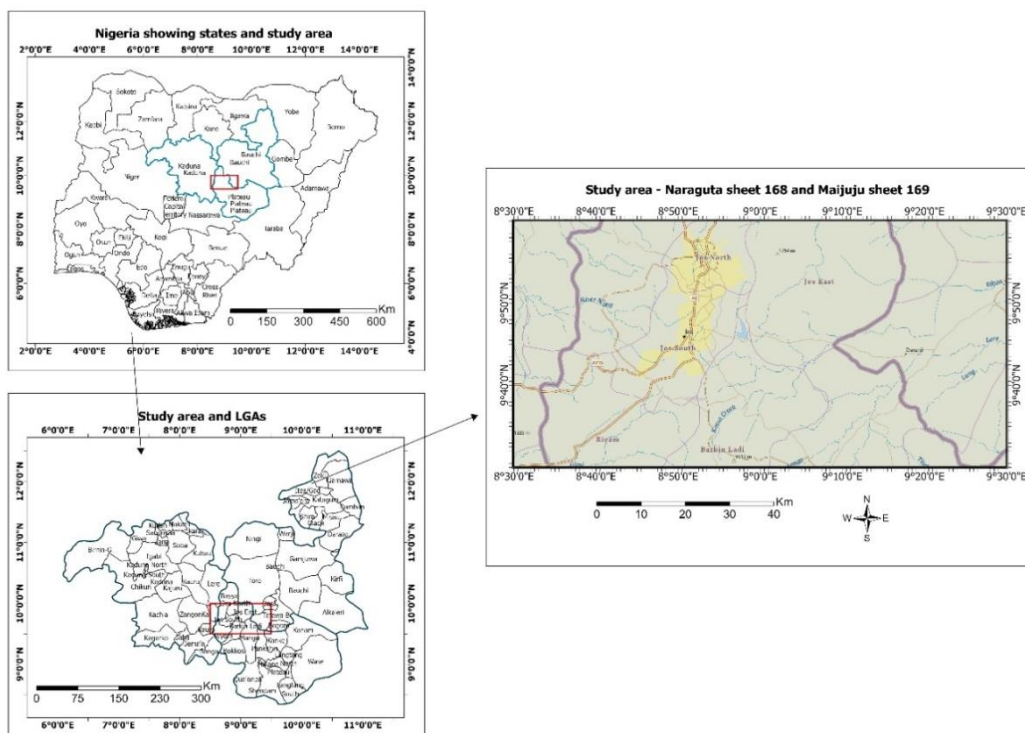


Figure 1. Location map of the study area projected from the administrative map of Nigeria.

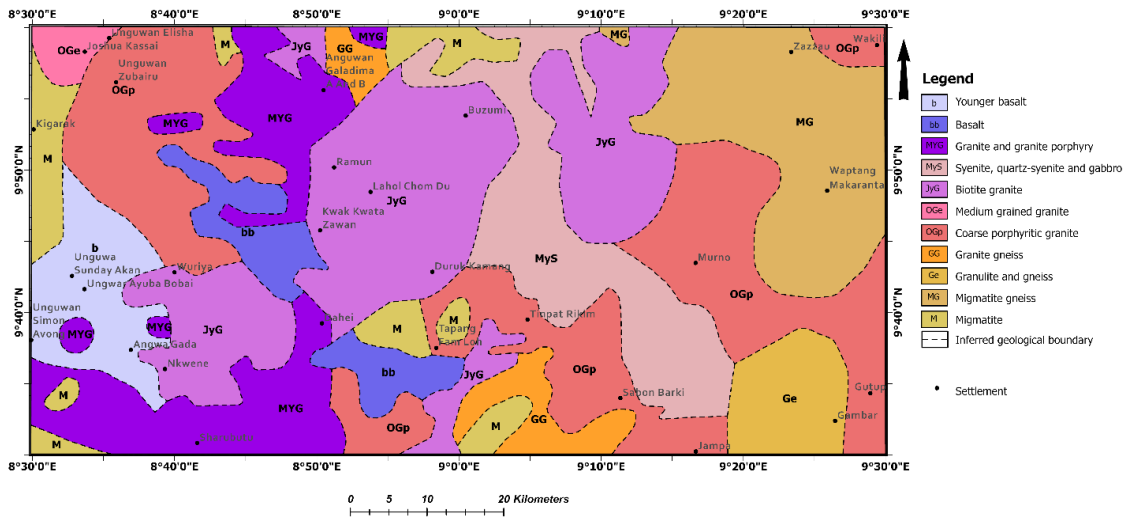


Figure 2. Map of Nigeria showing the study area; Naraguta sheet 168 and Maijuju Sheet 169 (Adapted from NGSA, 2009).

3. Methodology

3-1. Data Source and Survey Specifications

The high-resolution airborne geophysical data (magnetic and radiometric) covering the study area was obtained from the Nigerian Geological Survey Agency (NGSA) in Abuja. The various map sheets (sheets 168 and 169) were merged and processed together to create a common dataset. Table 1 shows the survey specifications used to acquire the data.

3-2. Theory of Method

3-2-1. Spectral Depth Analysis

The algorithm for the models of the centroid method employed the shape of an isolated magnetic anomaly, as described by Bhattacharyya and Leu (1975, 1977), and applied to the statistical properties of magnetic ensembles by Spector and Grant (1970). Blakely (1995) extended the same to

power spectral density of the magnetic field, $\phi\Delta T(k_x, k_y)$ as:

$$\phi\Delta T(k_x, k_y) = \phi_M(k_x, k_y) \cdot 4\pi^2 C_M^2 |\Theta_M|^2 |\Theta_f|^2 e^{-2|k|Z_t} (1 - e^{-2|k|(Z_b - Z_t)})^2 \tag{1}$$

k_x and k_y are wave numbers in x and y direction, $\phi_M(k_x, k_y)$ is power spectra of magnetization, C_M is a constant, Θ_M and Θ_f are magnetization and field direction, and Z_b and Z_t are depths to magnetic basement and of overburden layer respectively.

If the layer's magnetization, $M(x, y)$ is a random function of x, y it implies that $\phi_M(k_x, k_y)$ is a constant, and therefore the azimuthally averaged power spectrum, $\phi(|k|)$ would be given as:

$$\phi(|k|) = A e^{-2|k|Z_t} (1 - e^{-2|k|(Z_b - Z_t)})^2 \tag{2}$$

Table 1. Data Parameter and Specifications (NGSA, 2009).

Survey Parameter	Magnetic Specifications	Radiometric Specifications
Data Acquired by:	Fugro Airborne Surveys	Fugro Airborne Surveys
Time Range	2005 – 2009	2005 – 2009
Data Recording Interval	0.1 seconds or less	0.1 seconds or less
Sensor Mean Terrain Clearance	80 meters	80 meters
Flight Line Spacing	500 meters	500 meters
Tie Line Spacing	5000 meters	2000 meters
Flight Line trend	135 degrees	135 degrees
Tie Line trend	45 degrees	45 degrees
Equipment: Aircraft	Cessna Caravan 208B ZS-FSA, Cessna Caravan 208 ZS-MSJ	Cessna Caravan 208B ZS-FSA Cessna Caravan 208 ZS-MSJ
Equipment:	3 x Scintrex CS3 Cesium Vapour Magnetometer	(NaI “TI” crystals) 512-channels gamma-ray spectrometer

3-2-2. Depth to the Top (Z_t), Centroid (Z_0) and Bottom (Z_b) of Magnetic sources

Two approaches were employed here:

A) The depth to the top of the overburden is obtained from the slope of the high-wave-number portion of the power spectrum as:

$$\ln(P(k)^{\frac{1}{2}}) = A - |k|Z_t \quad (3)$$

where $P(k)$ is the azimuthally averaged power spectrum, k is the wave number ($2\pi \text{ km}^{-1}$), A is a constant, and Z_t is the depth to the top of magnetic sources.

B) The centroid depth, which comprises of both the overburden and the basement rocks, is obtained from the low-wave-number portion as (Tanaka et al., 1999):

$$\ln(P(k)^{\frac{1}{2}}/k) = B - |k|Z_0 \quad (4)$$

if B is a constant then Z_0 is the centroid, The depth of the magnetic source (Z_b) with a constant density and thermal conductivity of $2.5\text{W/m}^\circ\text{C}$ for granite required for evaluating the Geothermal Gradient can be obtained from the relation (Okubo et al., 1985; Adetona et al., 2017):

$$Z_b = 2Z_0 - Z_t \quad (5)$$

3-2-3. Geothermal Gradient and Heat Flow

Using the result of (Z_b), in Equation (7) above the geothermal gradient ($\frac{dT}{dz}$) can be estimated as

$$\left(\frac{dT}{dz}\right) = \left(\frac{\theta_c}{Z_b}\right); \quad (6)$$

where θ_c is the Curie temperature.

By employing, Z_b and $\frac{dT}{dz}$, the heat flow (q_z) can be estimated as (Okubo et al., 1985; Adetona et al., 2017)

$$q_z = -\sigma \left(\frac{\theta_c}{Z_b}\right) = -\sigma \left(\frac{dT}{dz}\right), \quad (7)$$

Where σ is thermal Conductivity, a value of $2.5\text{W/m}^\circ\text{C}$ as the average for igneous rocks and a Curie temperature of 580°C are used as standard (Stacey, 1977; Trifonova et al., 2009).

3-2-4. Estimating the Radiogenic Heat Production

Radiometric heat production (H) is primarily related to the decay of the radioactive isotopes ^{232}Th , ^{238}U and ^{40}K and can be

estimated based on the concentration (C) of the respective elements through the expression (Rybach, 1976; Birch, 1954):

$$H(\mu\text{W/m}^3) = \rho(0.0952 C_U + 0.0256 C_{Th} + 0.0348 C_K) \quad (8)$$

where; H = radioactive heat production ρ = density of rock adapted from (Telford et al., 1990; Madu et al., 2015). C_U , C_{Th} , C_K are concentrations of uranium, thorium and potassium, respectively. The concentration of the three radiometric elements is determined from the radiometric data, covering the study area.

3-3. Procedure

The total magnetic intensity data of the study area were divided into 16 overlapping blocks or sections, each consisting of 22.5 km^2 . Fast Fourier transform (FFT) was performed on each section using Oasis Montaj, and the data was extracted using Microsoft Excel. A plot of energy graphs against wave number in cycle/km for each section was done. A straight line was fitted to the energy spectrum for both the higher and the lower portion in an effort to determine the slope as well as the depth to the top (Z_t) and centroid (Z_0) of the magnetic sources. This implies that the depth to the top and centroid of the magnetic source was evaluated for every window 22.5 km apart. Figure 4 shows a sample graph of the logarithms of spectral energies for the blocks of the study area. The derived values for the depth to the top and centroid of the magnetic sources were used in the estimation of the Curie-point depth (Z_b), geothermal gradient and heat flow of the study area using Equations (5), (6) and (7). The estimated values of depth to centroid (Z_0), top (Z_t) and bottom (Z_b) of magnetic sources for the sixteen blocks are presented in Table 2.

Summarily, the depth to the base of the magnetic source (the Curie point depth) is calculated in four procedures (Tanaka et al., 1999) as follows:

A) Calculate the radially averaged power spectrum of the magnetic data in each window;

B) Estimate the centroid depth (Z_0) and depth to the top of the magnetic source (Z_t) using the low wave and high wave number portion of the magnetic anomaly power spectra;

C) Estimate the Curie depth, heat flow and geothermal gradient using Equations (5), (6) and (7), respectively.

Radiogenic heat production is obtained through the following procedure

A) Seven vertical profiles were drawn and plotted across the study area

B) Concentration of each radiometric elements (K, eTh and eU) at the midpoint of each section were recorded using sections map (Figure 3)

C) Using the concentration of each element, average density of the rock at the point and the radiogenic heat production of each section was evaluated using Equation (8).

4. Results and Discussion

4-1. Sectioned Total Magnetic Intensity Map

The total magnetic intensity map of the study area (Western part of Jos) in Nigeria consists of Naraguta (sheet 168) and Maijuju (sheet 169). The map was produced in color aggregate using Oasis Montaj as shown in Figure 3. The total magnetic intensity map of the study area exhibits both positive and negative anomalies, ranging from -159.1 nT to 113.3 nT. The positive (high) magnetic anomalies at Northern, Eastern and Western edge correspond to the crystalline rock, migmatit gneiss, porphyritic granite and granite gneiss.

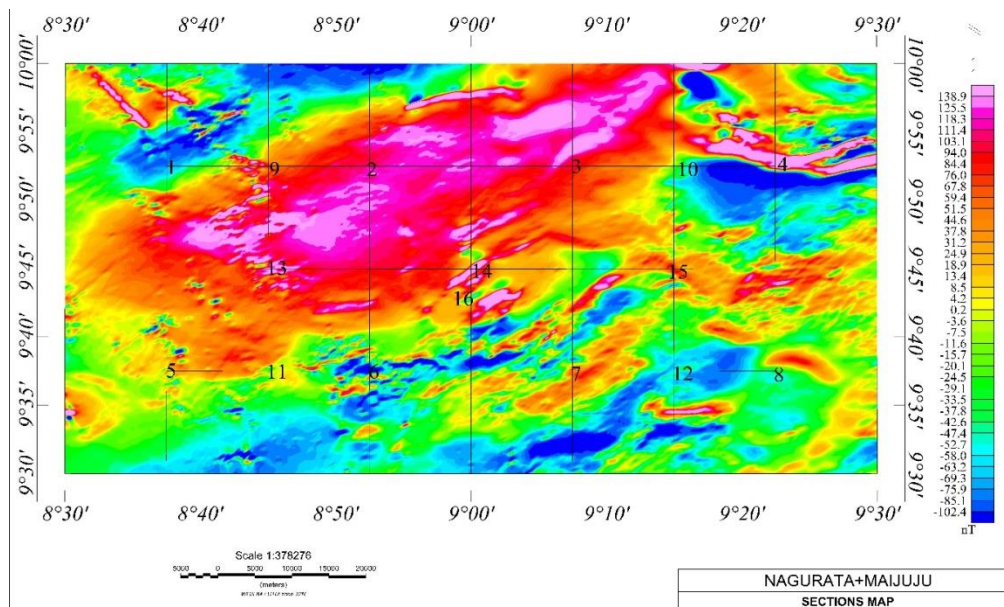


Figure 3. Sectioned Total Magnetic Intensity map of the study area

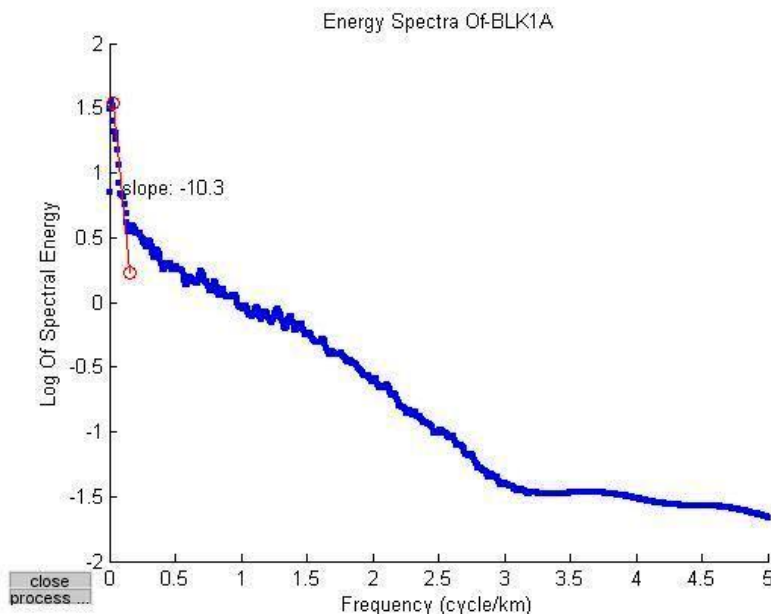


Figure 4. Graphs of the log of spectral energy against frequency for deep sources (spectral block 1).

4-2. Result of Curie Point Depth

The Curie point depth map of the study area is shown in Figure 5, which varies from 5 km to 74 km. High depth up to 74 km were recorded at the northern part of the study area, descending to 5 km at Western and South Eastern edge of the study area. The prominent areas that recorded high depth are situated at the North Eastern edge of the study area corresponding to Durbi, Shere, Nabatum, Daji and Katon Rikkos towns, respectively. Also, shallow Curie point depths were observed at the Western edge and South Eastern edge. These regions correspond to Pari, Manchok, Ataka, Gimi, Mongu, Kadunu and Jimjim towns, respectively.

4-3. Results of Heat Flow and Geothermal Gradient

Figure 6 depicts that the heat flow varies from 10 to 165.5 mW/m². High anomalous heat flow, ranging from 110 to 165.5 mW/m² is recorded in the study area. The most prominent high heat flow is situated at the South Eastern and Western edge of the study area. These regions correspond to Bawon Dodo, Gimi and Kaura town,

and this might occur as a result of high Uranium concentration, which was observed on a composite map in Figure 8. While the lowest heat flow was observed at the North Eastern edge of the study area corresponding to Durbi, Shere, Dan kurama and Angware towns, respectively. The geothermal gradient map (Figure 7) shows the variation of temperature with an increase in depth. The geothermal gradient varies from 8 to 66 °C/km with an average value of 26 °C/km. The regions with high geothermal gradients are situated at the Southern and Western edge of the study area. These regions correspond to Bawon Dodo, Gimi and Kaura town, and this may have occurred as a result of high Uranium concentration, which was observed on a composite map in Figure 8. While the lowest geothermal gradient was observed at the North central and Eastern edge of the study area corresponding to Durbi, Shere, Dan kurama and Angware towns respectively. Generally, the study area recorded an average heat flow of 65.40 mW/m², which is in agreement with summary of heat flow studies in Nigeria estimated by Akinyemi and Zui (2019).

Table 2. Estimated values of the Curie point depth, geothermal gradient and heat flow.

BLK	LON	LAT	Depth to Centroid Z ₀ (km)	Depth to Top Z _T (km)	Curie Point Depth Z _B (km)	Geothermal Gradient °C/km	Heat Flow mW/m ²
1	8.625	9.875	10.3	4.15	16.45	35.25835866	88.14589666
2	8.875	9.875	35.4	4.69	66.11	8.773256693	21.93314173
3	9.125	9.875	37.7	5.06	70.34	8.245663918	20.6141598
4	9.375	9.875	23.1	2.33	43.87	13.22087987	33.05219968
5	8.625	9.625	10.2	1.56	18.84	30.78556263	76.96390658
6	8.875	9.625	10.5	2.73	18.27	31.74603175	79.36507937
7	9.125	9.625	5.46	2.16	8.76	66.21004566	165.5251142
8	9.375	9.625	19.5	4.86	34.14	16.98886936	42.4721734
9	8.75	9.875	7.96	1.32	14.6	39.7260274	99.31506849
10	9.25	9.875	23.7	5.67	41.73	13.89887371	34.74718428
11	8.75	9.625	10.5	1.87	19.13	30.31887088	75.79717721
12	9.25	9.625	9.53	2.21	16.85	34.42136499	86.05341246
13	8.75	9.75	24.9	3.43	46.37	12.50808713	31.27021781
14	9.0	9.75	27.7	4.16	51.24	11.31928181	28.29820453
15	9.25	9.75	8.67	4.03	13.31	43.57625845	108.9406461
16	9.0	9.75	15.2	3.58	26.82	21.6256525	54.06413125

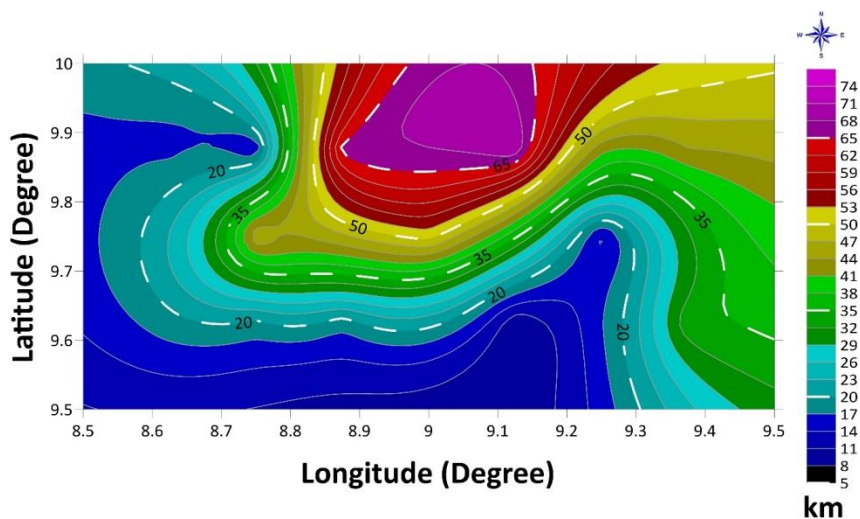


Figure 5. Curie point depth contour map of Naraguta and Maijuju.

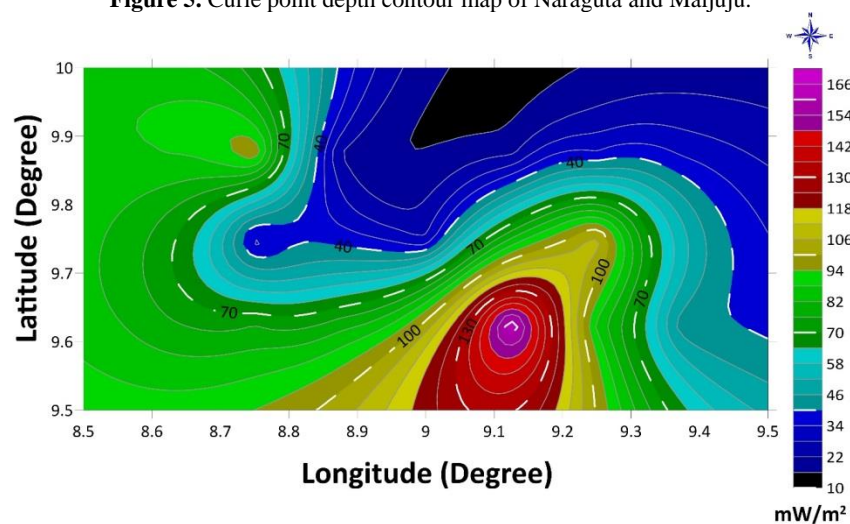


Figure 6. Heat flow contour map of Naraguta and Maijuju.

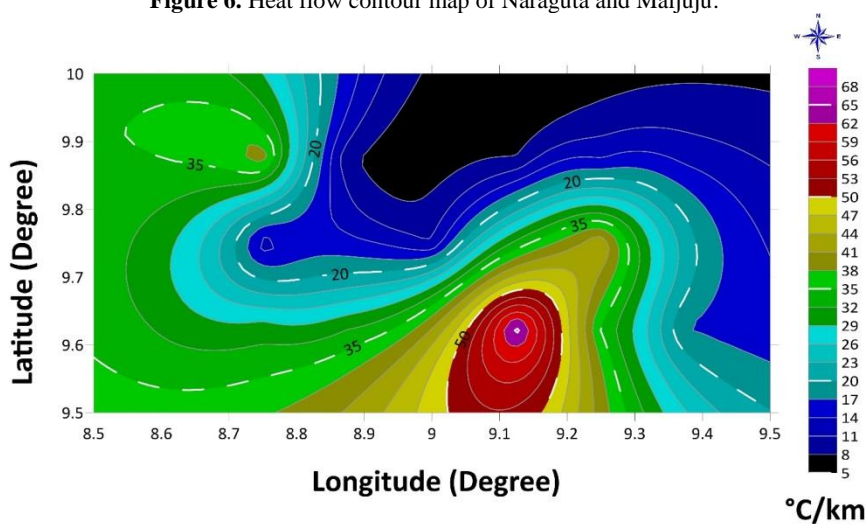


Figure 7. Geothermal gradient contour map of Naraguta and Maijuju.

4-4. Ternary map

The Ternary map is also the composite map for the three radiogenic elements (potassium, thorium and uranium). The map was produced by combination of the three

concentration maps for potassium, uranium and thorium representing red, blue and green coloration respectively. It revealed the slight variations in the radioelements concentration. In Figure 8, the white regions in the

composite map are indications of strong contents in potassium, uranium and thorium. The cyanide indicates strong content in thorium and uranium but weak potassium content. It is also observed that regions containing Granite and Biotite show red coloration, indicating strong content in potassium but weak in uranium and thorium. While the blue and dark blue regions marked within the study areas depicts strong content in uranium and it is located at the South East, South West and North Western edge of the study area. The regions depicting strong content of three elements namely potassium, thorium and uranium, correspond to high radiogenic heat production.

4-5. Radioelements concentration profiles map of study area

Radiogenic heat production of the study area

was obtained through the following procedure. Seven vertical profiles were drawn and plotted across the study area, to obtain the concentration of each radiometric element (K, eTh and eU) at the midpoint point of each section using a sectioned map (Figure 3). The profiles lines across study area are also outlined on the ternary map (Figure 8) as P1 to P7. The profiles map (Figure 9a and b) displayed three different color lines namely red, blue and green. This corresponds to three radiometric elements (K, eTh and eU). The concentration and rock unit corresponding to each radio element were recorded and indicated as shown on Figure 9(a and b). The average density of rock unit hosting these radiometric elements was used to calculate the Radiogenic Heat Production (RHP) at the midpoint of each section using Equation (8) as shown in Table 3.

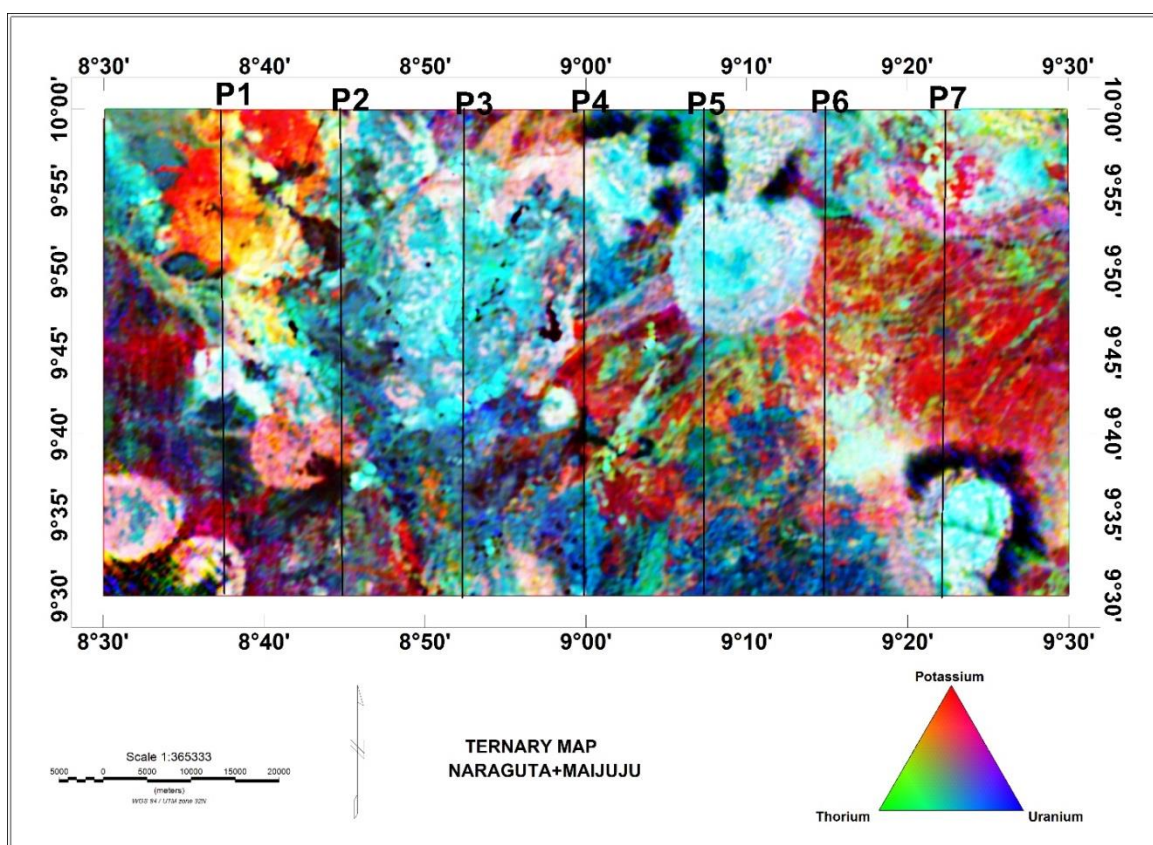


Figure 8. Ternary map of study area (with indicated profile lines P1 – P7).

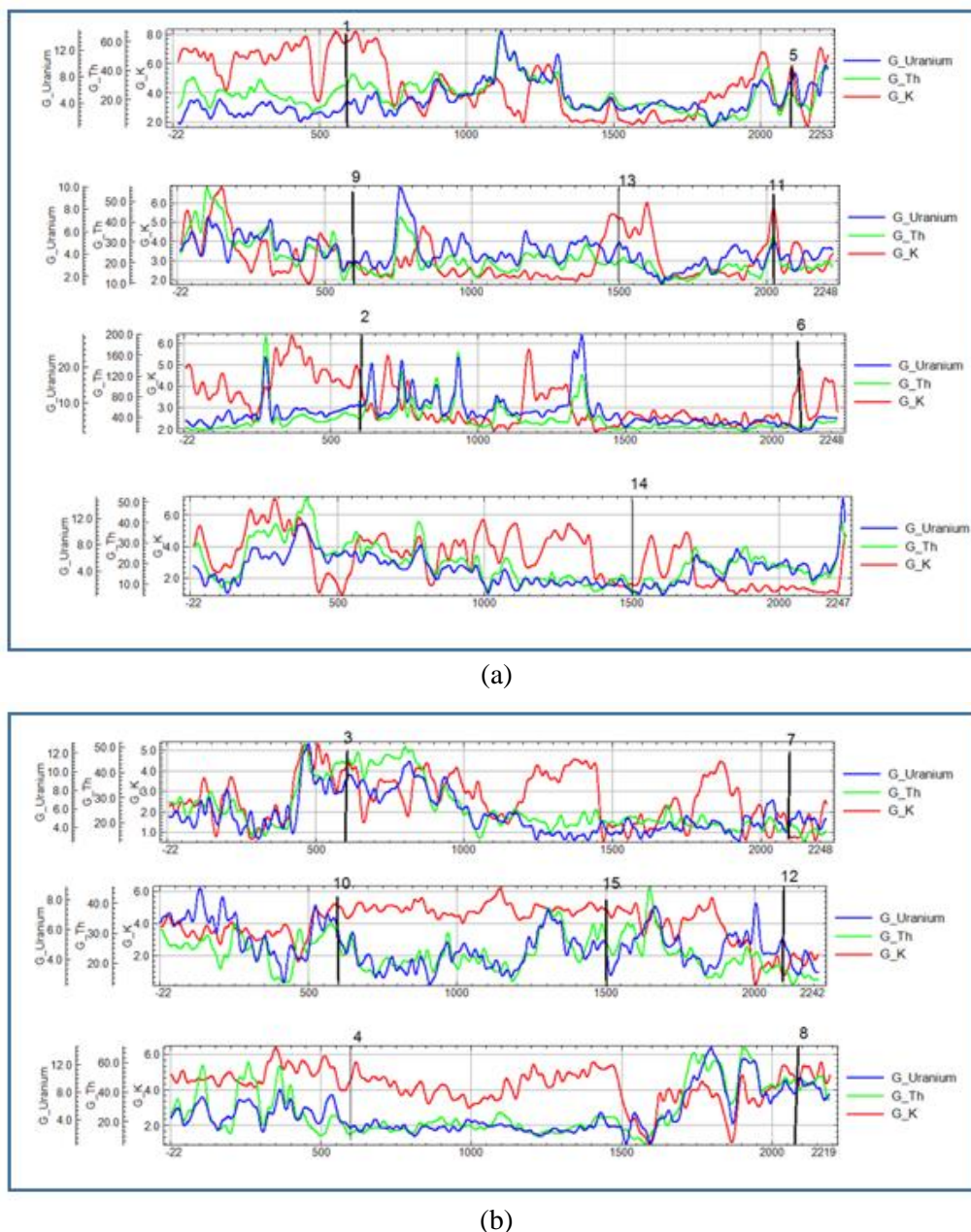


Figure 9. a) Profile 1 to 4 drawn across radiogenic elements in the study area, b) Profile 5 to 7 drawn across radiogenic elements in the study area.

Figure 9(a and b): Profiles Map for radio nuclide of potassium, thorium and uranium indicating concentration of each element used for calculating radiogenic heat production on Table 3.

4-6. Radiogenic Heat Production (RHP) Map

The summary table shown in Table 3 was used to produce a radiogenic heat production map (Figure 10) using Surfer version 16 contouring software. The map depicts the radiogenic heat values ranging from 0.4 $\mu\text{W}/\text{m}^3$ to 5.9 $\mu\text{W}/\text{m}^3$ with average

radiogenic heat value of 3.36 $\mu\text{W}/\text{m}^3$. The northern, Western edge and South Eastern corner of the study area depicts high radiogenic heat corresponding to coarse porphyritic biotite, migmatite, biotite granite and porphyry quartz. While the south - central depicts low radiogenic heat values and this corresponds to Basalts rock. In addition, research reveals that some granitic rocks are enriched in radioactive elements such as potassium, thorium and uranium and thus typically produce high heat. The basalt rock contains only a few radioactive elements (McCay et al., 2014; Megwara et al., 2013;

Abbady et al., 2006). Also in this study, the estimated radiogenic heat due to granitic rocks (3.4 to 5.9 $\mu\text{W}/\text{m}^3$) exceeds the average

content of $\sim 2.5 \mu\text{W}/\text{m}^3$ for granitic rocks and $\sim 0.9 \mu\text{W}/\text{m}^3$ for continental crust (Artemieva et al., 2017; Jaupart et al., 2016).

Table 3. Estimated values of the Radiogenic heat production.

Sections	Long	Lat	K	Th	U	Rock units	Av. Density g/cm^3	A ($\mu\text{W}/\text{m}^3$)
1	8.625	9.875	7.60	36.00	4.00	Porphyritic granite/coarse porphyritic Biotite	2.740	4.357
2	8.875	9.875	4.00	40.00	10.00	Biotite granite	2.650	5.698
3	9.125	9.875	4.20	44.00	10.00	Biotite granite	2.650	5.992
4	9.375	9.857	5.00	18.00	4.00	Porphyritic granite/coarse porphyritic Biotite	2.740	2.825
5	8.625	9.625	5.60	28.00	8.00	Biotite Granite	2.650	4.505
6	8.875	9.625	5.00	0.00	0.00	Basalts	2.990	0.523
7	9.125	9.625	1.20	24.00	6.00	Porphyritic granite/coarse porphyritic Biotite	2.740	3.420
8	9.375	9.625	4.00	44.00	8.00	Migmatite Gneiss	2.750	5.665
9	8.750	9.875	3.00	20.00	4.00	Basalts	2.990	3.029
10	9.250	9.875	5.00	30.00	6.00	Biotite granite	2.650	4.073
11	8.750	9.625	5.80	30.00	4.00	Younger Basalts	2.990	4.099
12	9.250	9.625	1.00	16.00	5.00	Granite Gneiss	2.770	2.593
13	8.750	9.750	5.20	2.00	4.00	Porphyritic granite/coarse porphyritic Biotite	2.740	1.704
14	9.000	9.750	1.60	4.00	1.60	Biotite Granite	2.650	0.835
15	9.250	9.750	4.50	28.00	5.00	Porphyry Quartz porphyry	2.650	3.632
16	9.000	9.750	1.60	4.00	1.60	Biotite Granite	2.650	0.835

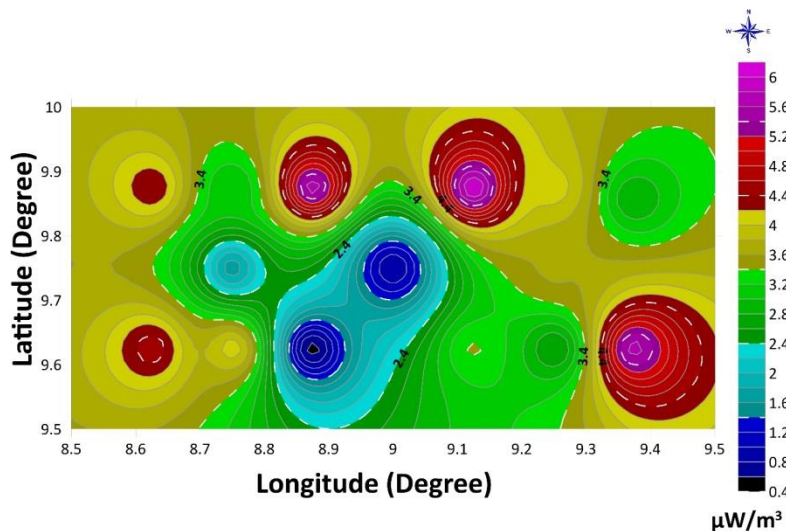


Figure 10. Radiogenic heat production map of the study area.

5. Conclusion

Curie-point depth contour map of the study area shows a depth range of 5 km to 74 km. High depth up to 74 km were recorded at the northern part of the study area, descending to 5 km at Western and South Eastern edge of the study area. Anomalous heat flow obtained within this study area ranges from 110 to 165.5 mW/m². This region also corresponds to the shallowest Curie point depth range of 5 to 11 km. The most prominent high heat flow is situated at the South Eastern and Western edge of the study area. These regions correspond to Pari, Manchok, Ataka, Gimi, Mongu, Kadunu, Dorowa Tsofo and Bawon Dodo towns. The towns with 80 to 100 mW/m² that are considered moderate for geothermal energy exploration were recorded at Vom, Wai, Kardam, Rafin Bauna, Badni, Boi, Mumo, BarkinKwi, Kuru, Lere, Bundia, and Bukuru. Also, a correlation of delineated geothermal parameters and radiogenic heat production across the study area can be clearly established. Correlating these two analyses, regions of anomalous high radiogenic heat production (4.4 to 5.9 $\mu\text{W}/\text{m}^3$) did not correspond to regions of anomalous high heat flow (110 to 165.5 mW/m²) as expected. The high concentration observed at these spots can be traced to human interference during mining and processing of mineral ores. Also, the high concentration of radio nuclei elements is measured at the shallow depth, since gamma ray's penetration through materials (rocks and air) are usually below 1 m (0-0.5 m) (McCay et al., 2014). Spots where anomalous high heat flow and high radiogenic heat production values were observed are Bawon Dodo, Mongu, Kassa, Durbi, Shere and Jos. They are dominated by the following rock types that host the radio elements; biotite granite and granite porphyry. However, the two methods depict the same suitable region for safe geothermal exploration and the regions include Ataka, Gimi, Jimjim and Pari.

References

- Abbadly, A. G., El-Arabi, A. M., & Abbadly, A. (2006). Heat production rate from radioactive elements in igneous and metamorphic rocks in Eastern Desert, Egypt. *Applied radiation and isotopes*, 64(1), 131-137.
- Adagunodo, T. A., Bayowa, O. G., Usikalu, M. R., & Ojoawo, A. I. (2019). Radiogenic heat production in the coastal plain sands of Ipokia, Dahomey Basin, Nigeria. *MethodsX*, 6, 1608-1616.
- Adetona, A. A., Salako, K. A., Rafiu A. A. (2017). Curie Depth and Geothermal Gradient from spectral analysis of aeromagnetic data over upper Anambra and lower Benue Basin, Nigeria. *Nigeria Journal of Technological Research (NJTR)*, 12(2), 20-26, DOI:<https://dx.doi.org/10.4314/njtr.v12i2.4>.
- Adetona, A. A., Fidelis, I. K., & Shakirat, B. A. (2023). Interpreting the magnetic signatures and radiometric indicators within Kogi State, Nigeria for economic resources. *Geosystems and Geoenvironment*, 2(2), 100157, <https://doi.org/10.1016/j.gegeo.2022.100157>.
- Akinyemi, L., & Zui, V. I. (2019). Summary of heat flow studies in Nigeria.
- Artemieva, Irina M., Hans Thybo, Kiki Jakobsen, Nanna K. Sørensen, and Louise SK Nielsen (2017). Heat production in granitic rocks: Global analysis based on a new data compilation GRANITE2017. *Earth-Science Reviews*, 172, 1-26.
- Bhattacharyya, B. K., & Leu, L. K. (1977). Spectral analysis of gravity and magnetic anomalies due to rectangular prismatic bodies. *Geophysics*, 42(1), 41-50.
- Bhattacharyya, B. K., & Leu, L. K. (1975). Spectral analysis of gravity and magnetic anomalies due to two-dimensional structures. *Geophysics*, 40(6), 993-1013.
- Birch, F. (1954). Heat from radioactivity. *Nuclear geology*, 148, 174.
- Blakely, R. J. (1995). Potential theory in gravity and magnetic applications. Cambridge University Press, Cambridge.
- Cull, J. P., & Conley, D. (1983). Geothermal gradients and heat flow in Australian sedimentary basins. *Geoscience Australia, Canberra*. Record 8(4), 329-337. <http://pid.geoscience.gov.au/dataset/ga/81160>.
- Davies, G. F. (1980). Thermal histories of convective Earth models and constraints on radiogenic heat production in the Earth. *Journal of Geophysical Research: Solid Earth*, 85(B5), 2517-2530.
- Jaupart, C., Mareschal, J. C., & Iarotsky, L.

- (2016). Radiogenic heat production in the continental crust. *Lithos*, 262, 398-427.
- Jessop, A. M., Habart, M. A., & Sclater, J. G. (1976). The world heat flow data collection 1975. Geothermal services of Canada. *Geothermal Series*, 50, 55-77.
- Kuforijimi, O., & Aigbogun, C. (2017). Assessment of aero-radiometric data of Southern Anambra Basin for the prospect of radiogenic heat production. *Journal of Applied Sciences and Environmental Management*, 21(4), 743-748.
- Lowrie, W., & Fichtner, A. (2020). *Fundamentals of geophysics*. Cambridge University Press.
- Madu, A.J.C., Amoke, A.I., & Onuoha, M.K., (2015). Density and Magnetic Susceptibility Characterization in the Basement Complex Terrain of NE Kogi State/NW Benue State of Nigeria. *International Journal of Science and Research (IJSR)*, 5(12).
- McCay, A.T., Harley, T.L., Younger, P.L., Sanderson, D.C. & Cresswell, A.J. (2014). Gamma-ray spectrometry in geothermal exploration: State of the art techniques. *Energies*, 7(8), 4757-4780.
- Macleod, W. N., Turner, D. C., & Wright, E. P. (1971). The Geology of Jos Plateau. *Geological Survey of Nigeria*, 32(1-2).
- Maden, N. (2010). Curie-point depth from spectral analysis of magnetic data in Erciyes stratovolcano (Central TURKEY). *Pure Applied Geophysics*, 167, 349-358.
- Megwara, J. U., Udensi, E. E., Olasehinde, P. I., Daniyan, M. A., & Lawal, K. M. (2013). Geothermal and radioactive heat studies of parts of southern Bida basin, Nigeria and the surrounding basement rocks. *Int J Basic Appl Sci*, 2(1), 125-139.
- Nagata, T. (1961). *Rock magnetism*. Tokyo, Maruzen Company Tokyo.
- NGSA. (2009). Airborne geophysical survey specifications, Nigeria Geological Survey Agency, <https://ngsa.gov.ng/geological-maps>.
- Nuri, D. M., Timur, U. Z., Mumtaz, H., & Naci, O. (2005). Curie Point Depth variations to infer thermal structure of the crust at the African-Eurasian convergence zone, SW Turkey. *Journal of Earth planets Space*, 57, 373-383.
- Nwankwo, L. I., Olasehinde, P. I., & Akoshile, C. O. (2009). An attempt to estimate the Curie-point isotherm depths in the Nupe Basin, West Central Nigeria. *Global Journal of Pure and Applied Science*, 15, 427433.
- Nwankwo, L. I., & Sunday, A. J. (2017). Regional estimation of Curie-point depths and succeeding geothermal parameters from recently acquired high-resolution aeromagnetic data of the entire Bida Basin, north-central Nigeria. *Geothermal Energy Science*, 5(1), 1.
- Obaje, N. G. (2009). Geology and Mineral Resources of Nigeria, London: *Springer Dordrecht Heidelberg*, 5-14.
- Okubo, Y., Graff, R. G., Hansen, R. O., Ogawa, K., & Tsu, H. (1985). Curie point depths of the Island of Kyushu and surrounding areas, *Geophysics*, 53, 481-494.
- Raj, K., Bansal, A., & Abdolreza, G. (2020). Estimation of Depth to Bottom of Magnetic Sources Using Spectral Methods: Application on Iran's Aeromagnetic Data. *Journal of Geophysical Research: Solid Earth*, 125(3).
- Rybach, L., (1976). Radioactive heat production: A physical property determined by the chemistry of rocks. In *The Physics and Chemistry of Minerals and Rocks*; Stems, R.G.J., Ed.; *Wiley-Interscience*: New York, USA, 1976; 309-318.
- Salako, K.A., Adetona, A.A., Rafiu, A.A., Alahassan, U.D., Aliyu, A., & Adewumi, T. (2020). Assessment of geothermal potential of parts of middle Benue Trough, North-East Nigeria. *J. Earth Space Phys.*, 45(4), doi: 10.22059/jesphys.2019.260257. 1007017.
- Spector, A., & Grant, F. S. (1970). Statistical models for interpreting aeromagnetic data. *Geophysics*, 35, 293- 302.
- Stacey, F. D. (1977). A thermal model of the Earth. *Physics of the Earth and Planetary Interiors*, 15(4), 341-348.
- Tanaka, A. Y., Okubo, Y., & Matsubayashi, O. (1999). Curie point depth based on spectrum analysis of the magnetic anomaly data in East and Southeast Asia. *Tectonophysics*, 306, 461-470.
- Telford, W. M., Geldart, L. P., Sherif, R. E., & Keys, D. A. (1990). *Applied Geophysics*. Cambridge: Cambridge University Press.

Trifonova, P., Zhelev, Z., Petrova, T., & Bojadgieva, K. (2009). Curie point depth of Bulgarian territory inferred from geomagnetic observations and its correlation with regional thermal structure and seismicity. *Tectonophysics*, 473, 362–374.